

See discussions, stats, and author profiles for this publication at: <https://www.researchgate.net/publication/256118488>

Speciation of Platinum(IV) in Nitric Acid Solutions

ARTICLE *in* INORGANIC CHEMISTRY · AUGUST 2013

Impact Factor: 4.76 · DOI: 10.1021/ic401499j · Source: PubMed

CITATIONS

5

READS

115

4 AUTHORS, INCLUDING:



[Sergey Victorovich Tkachev](#)

Russian Academy of Sciences

64 PUBLICATIONS 334 CITATIONS

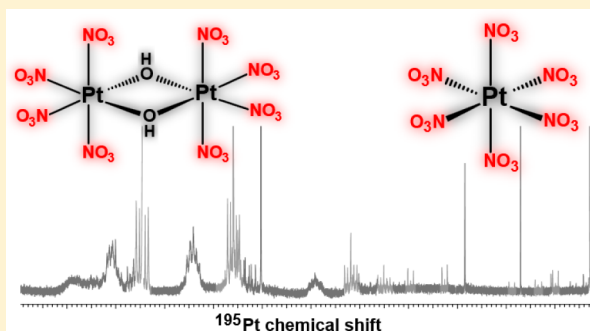
SEE PROFILE

Speciation of Platinum(IV) in Nitric Acid Solutions

Danila Vasilchenko,^{*,†,‡} Sergey Tkachev,[†] Iraida Baidina,[†] and Sergey Korenev^{†,‡}[†]Nikolaev Institute of Inorganic Chemistry, Siberian Branch of the Russian Academy of Science, Novosibirsk 630090, Russia[‡]Novosibirsk State University, Novosibirsk 630090, Russia

S Supporting Information

ABSTRACT: The speciation of platinum(IV) ions in nitric acid (6–15.8 M) solutions of $\text{H}_2[\text{Pt}(\text{OH})_6]$ has been studied by ^{195}Pt NMR and Raman spectroscopy. Series of aqua-hydroxo-nitrato complexes $[\text{Pt}(\text{L})_x(\text{NO}_3)_{6-x}]$ ($\text{L} = \text{H}_2\text{O}$ or OH^- ; $x = 0, \dots, 6$) were found to exist in such solutions. The pair additivity model of chemical shifts and statistical theory were used to assign signals in NMR spectra to particular $[\text{Pt}(\text{L})_x(\text{NO}_3)_{6-x}]$ species. Mononuclear hexanitratoplatinates(IV) have been isolated in solid state in substantial yield as pyridinium salt $(\text{PyH})_2[\text{Pt}(\text{NO}_3)_6]$ and characterized by single-crystal X-ray diffraction. Aging of the platinum nitric acid solutions for more than 5–6 h results in oligomerization of $[\text{Pt}(\text{L})_x(\text{NO}_3)_{6-x}]$ species and the formation of oligonuclear aqua-hydroxo-nitrato complexes with OH^- and NO_3^- bridging ligands. Oligomeric platinum(IV) complexes with two and four nuclei were unambiguously detected by NMR on ^{195}Pt -enriched samples. Oligomers with even higher nuclearity were also detected. Dimeric anions $[\text{Pt}_2(\mu\text{-OH})_2(\text{NO}_3)_8]^{2-}$ have been isolated as single crystals of tetramethylammonium salt and characterized by X-ray diffraction.



INTRODUCTION

The lability of metal complexes with nitrate ions is a reason of its common usage as a starting material for synthesis of coordination compounds with different types of ligands. On the other hand, without competing ligands in solutions, nitrate complexes are sufficiently stable and demonstrate versatile chemistry.^{1–10}

There is particular interest to nitrato complexes in noble-metals chemistry, because such compounds are labile (especially thermolabile) precursors of noble-metal particles for heterogeneous catalysis.¹¹ In addition, nitrato complexes play a crucial role in extraction technology of platinum metals recovery from spent nuclear fuel.^{12,13}

The pioneer work of Addison¹⁴ and similar works of Harrison and Wickleder created and developed method of preparation for noble-metal complexes with only nitrate ions as ligands by interaction of nitrogen oxides (N_2O_5 , N_2O_4) with metals and their compounds.^{15–17} Different approach is isolation of such compounds from water or organic solution containing excess of HNO_3 or nitrate salts. This way requires detailed knowledge about metals behavior and speciation under given conditions.

Platinum(II) complexes with nitrate-ions were studied by NMR technique by Appleton and co-workers.¹⁸ They have identified aqua-nitrato complexes $[\text{Pt}(\text{H}_2\text{O})_{4-x}(\text{NO}_3)_x]^{2-x}$ in nitric acid solutions of $\text{Pt}(\text{OH})_2 \cdot 2\text{H}_2\text{O}$. From such solutions, crystals of $\text{K}_2[\text{Pt}(\text{NO}_3)_4]$ were grown and structure of $[\text{Pt}(\text{NO}_3)_4]^{2-}$ anion with four monodentate NO_3^- ligands was determined.¹⁹ The approach developed in the aforemen-

tioned works can be modified and adapted for the preparation of Pt(IV) nitrate complexes.

There are little data about the complexation of platinum(IV) in nitric acid solutions. The dissolution of $\text{H}_2[\text{Pt}(\text{OH})_6]$ ($[\text{Pt}(\text{H}_2\text{O})_2(\text{OH})_4]^{20}$) in concentrated HNO_3 leads to so-called “platinum nitrate” (CAS No. 18496-40-7) of uncertain nature, widely used for the preparation of heterogeneous catalysts.^{21–27}

Mononuclear and polynuclear complexes of Pt(IV) with octahedral oxygen environment had been postulated to exist in such solutions according to EXAFS data.^{28–30} The ^{195}Pt NMR exploration confirmed a hypothesis about the presence of two sets of complexes (mononuclear and polynuclear) with OH^- , H_2O , and NO_3^- ligands but detailed pattern of Pt(IV) complexation and polynuclear complexes structure was unclear.^{31,32}

In the present work, we report new data about the speciation of Pt(IV) in concentrated nitric acid (6–15.8M) solutions obtained by means of ^{195}Pt NMR and Raman spectroscopy, as well as crystal structures of new $[\text{Pt}(\text{NO}_3)_6]^{2-}$ and $[\text{Pt}_2(\mu\text{-OH})_2(\text{NO}_3)_8]^{2-}$ complexes.

EXPERIMENTAL SECTION

General Procedures. Hexachloroplatinic acid produced at “The Gulidov Krasnoyarsk Non-Ferrous Metals Plant” of the Open Joint Stock Company, with a platinum content of 39.1%, was used as a starting reagent for the synthesis of $\text{H}_2[\text{Pt}(\text{OH})_6]$. Isotopically

Received: June 14, 2013



Table 1. Crystal Data and Experimental Details for $(\text{PyH})_2[\text{Pt}(\text{NO}_3)_6]$ and $(\text{Me}_4\text{N})_2[\text{Pt}_2(\mu\text{-OH})_2(\text{NO}_3)_8]$

parameter	$(\text{PyH})_2[\text{Pt}(\text{NO}_3)_6]$	$(\text{Me}_4\text{N})_2[\text{Pt}_2(\mu\text{-OH})_2(\text{NO}_3)_8]$
stoichiometric formula	$\text{C}_{10}\text{H}_{12}\text{N}_8\text{O}_{18}\text{Pt}$	$\text{C}_4\text{H}_{12}\text{N}_5\text{O}_{13}\text{Pt}$
formula weight	727.33	533.28
temperature (K)	150(2)	150(2)
wavelength (Å)		0.71073
crystal system	monoclinic	monoclinic
space group	$P2_1/c$	$P2_1/c$
unit-cell dimensions		
<i>a</i> (Å)	7.7948(4)	7.6907(3)
<i>b</i> (Å)	17.2938(8)	14.8950(5)
<i>c</i> (Å)	8.0747(4)	13.1091(4)
β (°)	98.569(1)	104.169(1)
volume (Å ³)	1076.33(9)	1456.00(9)
<i>Z</i>	2	4
absorption coefficient (mm ^{−1})	6.627	9.718
<i>D</i> _{calc} (g cm ^{−3})	2.244	2.433
<i>F</i> (000)	700	1012
θ range for data collection (°)	2.36–31.63	2.11–31.97
limiting indices	−11 ≤ <i>h</i> ≤ 11, −25 ≤ <i>k</i> ≤ 25, −11 ≤ <i>l</i> ≤ 11	−11 ≤ <i>h</i> ≤ 11, −17 ≤ <i>k</i> ≤ 22, −11 ≤ <i>l</i> ≤ 19
reflections collected	14130	12154
independent reflections	3606 [<i>R</i> (int) = 0.0130]	5035 [<i>R</i> (int) = 0.0206]
completeness (%)	99.9	99.8
max. and min. transmission	0.4572 and 0.2411	0.6972 and 0.4750
refinement method		full-matrix least-squares on <i>F</i> ²
data/parameters	3606/194	5035/224
goodness-of-fit on <i>F</i> ²	1.199	0.991
final <i>R</i> indices [<i>I</i> > 2σ(<i>I</i>)]	<i>R</i> 1 = 0.0196, <i>wR</i> 2 = 0.0357	<i>R</i> 1 = 0.0194, <i>wR</i> 2 = 0.0407
<i>R</i> indices (all data)	<i>R</i> 1 = 0.0242, <i>wR</i> 2 = 0.0367	<i>R</i> 1 = 0.0259, <i>wR</i> 2 = 0.0419
CCDC No.	926762	929104

enriched Pt powder (“Izotop” Open Joint Stock Company, 85% ¹⁹⁵Pt) was dissolved in aqua regia and evaporated thrice with the addition of hydrochloric acid to produce isotopically enriched hexachloroplatinic acid. Nitric acid (15.8 M concentration was determined by acid–base titration), perchloric acid (9.3M), sodium hydroxide, tetramethylammonium nitrate (96%, Sigma–Aldrich), and pyridine (99+%, Sigma–Aldrich), were all of reagent-grade quality and used without further purification. The acids solutions with different concentration were prepared by accurate dilution of the stock solutions.

NMR Data Collection. ¹⁹⁵Pt NMR spectra were recorded at 107.5 MHz using an Avance III 500 Bruker spectrometer with a 5-mm broadband probe. A 90° excitation pulse of 15 μs was applied. All spectra were recorded at 24 °C, unless otherwise stated. δ¹⁹⁵Pt (ppm) are reported relative to the external reference: a 2 M solution of H₂[PtCl₆] in 1 M hydrochloric acid. The usual spectral window of 67 kHz (620 ppm) was used with an acquisition time of 0.1 s and a pulse delay of 0.7 s to allow ¹⁹⁵Pt nuclei to relax completely. The time dependence of platinum speciation in the solutions was determined in the ¹⁹⁵Pt NMR experiment, using the following parameters: spectral window, 120 kHz (1100 ppm); acquisition time, 0.3 s; and pulse delay, 0.5 s. In addition, 160 FIDs were accumulated for every time point. A line-broadening factor of 1 Hz was applied when processing all of the experimental FID data. Areas of signals located far from the transmitter offset may not accurately reflect the concentration; nevertheless, they may serve as a relative indication of the species real fractions.

Raman Scattering Spectra. Raman scattering spectra were measured on a Triplemate SPEX spectrometer that was equipped with a CCD camera and microscope for detection of the back-scattering spectra with excitation by a 488-nm laser line.

X-ray Phase Analysis. X-ray phase analysis of the polycrystalline samples was carried out on a DRON-RM4 diffractometer (Cu *K*α radiation, using a graphite monochromator in the reflected beam, and a scintillation detector with amplitude discrimination). The samples were prepared by applying a suspension in hexane on the polished side

of the cell made of fused quartz. A sample of polycrystalline silicon (*a* = 5.4309 Å), prepared similarly, was used as an external standard. Indexing of the diffraction patterns for the compounds was carried out using the data reported in the PDF database.³³

Crystal Structure Determination. Crystal data and experimental details for $(\text{PyH})_2[\text{Pt}(\text{NO}_3)_6]$ and $(\text{Me}_4\text{N})_2[\text{Pt}_2(\mu\text{-OH})_2(\text{NO}_3)_8]$ are given in Table 1. Experimental data for determination of the crystal structures were collected on a Bruker-Nonius X8 APEX CCD diffractometer at a temperature of 150 K, using graphite-monochromated Mo *K*α radiation (*λ* = 0.7107 Å). All calculations were carried out with SHELX-97 crystallographic software package.³⁴ The structure was solved by the standard heavy atom method and refined in the anisotropic approximation. The H atoms were refined in their geometrically calculated positions; a riding model was used for this purpose. Absorption corrections were applied empirically with the SADABS program.³⁵

Preparation of Na₂[Pt(OH)₆]. To a solution of 2.44 g H₂PtCl₆·*x*H₂O (4.9 mmol of Pt) in H₂O (6 mL) was added 6.46 g (160 mmol) of solid NaOH. The resulting orange solution was boiled for 1 h and then cooled to room temperature. Pale yellow precipitate of Na₂Pt(OH)₆ was filtered off, washed with a minimal volume of ice water and 50 mL of methanol, and then dried in a stream of air. Yield: 1.47 g (87%). Anal. Calcd for H₆Na₂O₆Pt: H, 4.10; Na, 13.1. Found: H, 3.88; Na, 13.40.

Preparation of H₂[Pt(OH)₆]. To a solution of 1.47 g (4.3 mmol) of Na₂[Pt(OH)₆] in 35 mL of H₂O was added diluted HNO₃ (2 M) up to pH 3. Pale yellow precipitate was filtered off, washed with a 1 × 10^{−3} M solution of HNO₃ (30 mL), water (10 mL), and acetone (10 mL), and then dried in a stream of air. Yield: 95%. Anal. Calcd for H₈O₆Pt: Pt, 34.79. Found: Pt, 34.9.

Samples of synthesized H₂[Pt(OH)₆] and Na₂[Pt(OH)₆] were single phase (as determined via X-ray phase analysis) and their diffraction patterns clearly matched the diffraction data for corresponding compounds in the PDF database (see JCPDS File Nos. 32-439 and 29-1453).

Dissolution of $\text{H}_2[\text{Pt}(\text{OH})_6]$ in Nitric Acid (Preparation of "Platinum Nitrate" Solution). A sample of $\text{H}_2[\text{Pt}(\text{OH})_6]$ (150 mg, 0.5 mmol) was mixed with 2 mL of HNO_3 (15.8 M or any desired concentration). The temperature of the mixture was maintained at ~ 0 – 5°C with an ice bath until full dissolution (1–2 min). A portion (0.7 mL) of the resulting solution was transferred into an NMR tube. The rest of the solution was used for Raman spectroscopy experiments or analytical determination of the platinum content. For preparation of the samples with different platinum concentration, an identical procedure was used, differing only in the amount of $\text{H}_2[\text{Pt}(\text{OH})_6]$. The solutions of $\text{H}_2[\text{Pt}(\text{OH})_6]$ in HClO_4 and H_2SO_4 were prepared analogously.

Preparation of $(\text{PyH})_2[\text{Pt}(\text{NO}_3)_6]$. Solution of $\text{H}_2[\text{Pt}(\text{OH})_6]$ (150 mg, 0.5 mmol) in 2 mL of a HNO_3 – H_2O – Py mixture (1:2:0.1 molar ratio) was allowed to stand in a desiccator under solid KOH at room temperature. After 5 days, pale yellow prisms were filtered out, washed with a minimal volume of 15.8 M HNO_3 and acetone, and dried in a stream of air. Yield: 48%. Anal. Calcd for $\text{C}_{10}\text{H}_{12}\text{N}_8\text{O}_{18}\text{Pt}$: C, 16.51; H, 1.66; N, 15.41. Found: C, 16.6; H, 1.7; N, 15.3. Single crystals for X-ray analysis were extracted from the mother liquor.

Preparation of $(\text{Me}_4\text{N})_2[\text{Pt}_2(\mu\text{-OH})_2(\text{NO}_3)_6]$. Solution of $\text{H}_2[\text{Pt}(\text{OH})_6]$ (150 mg, 0.5 mmol) in 2 mL of HNO_3 – H_2O – $(\text{Me}_4\text{N})\text{NO}_3$ mixture (1:2:0.1 molar ratio) was allowed to stand in a desiccator under solid KOH at room temperature. After 5 days, yellow prisms were filtered out, washed with a minimal volume of 15.8 M HNO_3 and acetone, and dried in a stream of air. Yield: 40%. Anal. Calcd for $\text{C}_8\text{H}_{26}\text{N}_{10}\text{O}_{26}\text{Pt}_2$: C, 8.99; H, 2.45; N, 13.11. Found: C, 8.8; H, 2.4; N, 12.9. Single crystals for X-ray analysis were collected from the mother liquor.

RESULTS AND DISCUSSION

Acid Solutions of $\text{H}_2[\text{Pt}(\text{OH})_6]$. Dissolving of $\text{H}_2[\text{Pt}(\text{OH})_6]$ in concentrated acids leads to yellow solutions containing aqua-hydroxo complexes of platinum(IV). Because of a fast proton exchange, only one averaged signal from the $[\text{Pt}(\text{H}_2\text{O})_x(\text{OH})_{6-x}]^{x-2}$ mixture is exhibited in the range 3300–3400 ppm of ^{195}Pt NMR spectra. Figure 1 shows the

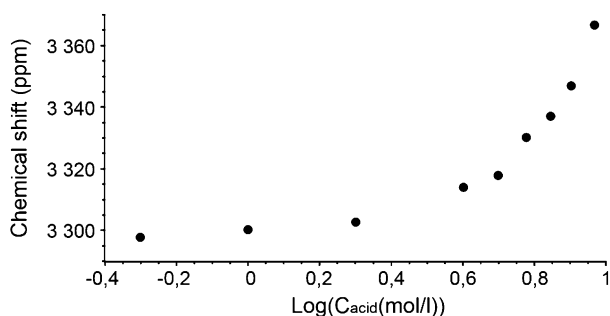


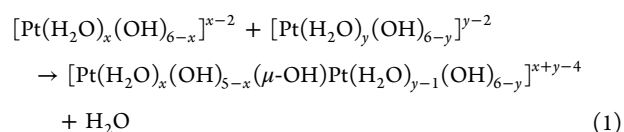
Figure 1. Plot of ^{195}Pt NMR chemical shift (ppm) of $[\text{Pt}(\text{H}_2\text{O})_x(\text{OH})_{6-x}]^{x-2}$ complex in HClO_4 solution versus the logarithm of the acid concentration. All measurements carried out at an ionic strength of 9.3 M, maintained with NaClO_4 .

dependence of the ^{195}Pt chemical shift on the concentration of perchloric acid in the solutions at constant ionic strength (ionic strength of the solution was kept constant by addition of NaClO_4). Increase in the acidity leads to a downfield shift of the signal as a result of the complex protonation. However, complete conversion into $[\text{Pt}(\text{H}_2\text{O})_6]^{4+}$ cannot be achieved under given conditions (conc. HClO_4 , HNO_3).

Solutions of $\text{H}_2[\text{Pt}(\text{OH})_6]$ in 0.5–5 M acids (HClO_4 , HNO_3) are unstable and produce an orange solid product insoluble in concentrated HClO_4 , HNO_3 , but readily soluble in hydrochloric acid with the formation of $[\text{PtCl}_6]^{2-}$ species. IR spectra of the solid products precipitated from HClO_4 or

HNO_3 solutions do not contain bands of corresponding (ClO_4^- , NO_3^-) anions. Analogous orange product was obtained by hydrolysis of platinum(IV) complexes in "nitrate solutions" and was described as $\text{PtO}_2 \cdot 3\text{H}_2\text{O}$.¹⁸

We supposed that at a "low" concentration of acids (0.5–5 M), complex species $[\text{Pt}(\text{H}_2\text{O})_x(\text{OH})_{6-x}]^{x-2}$ having a charge of 0, ..., +2 ($x = 2, \dots, 4$) predominate and can participate in the oligomerization process, leading to OH-bridged complexes:



Further condensation of platinum(IV) aqua-hydroxo complexes leads to insoluble $\text{PtO}_2 \cdot 3\text{H}_2\text{O}$. The rate of condensation depends on the acid concentration: 0.5–1 M solutions precipitate $\text{PtO}_2 \cdot 3\text{H}_2\text{O}$ after several hours while in 4–5 M solutions, precipitation is observed only after 1–2 days.

On the other hand, in more-acidic solutions highly charged (+2, ..., +4) species $[\text{Pt}(\text{H}_2\text{O})_x(\text{OH})_{6-x}]^{x-2}$ ($x = 4, \dots, 6$) predominate. Their aggregation seems hindered from an electrostatic point of view, and solutions of $\text{H}_2[\text{Pt}(\text{OH})_6]$ in acids with concentrations of more than 6 M were stable in an observable period (three months).

These suggestions correlate well with results of early examination of $\text{H}_2[\text{Pt}(\text{OH})_6]$ solutions in sulfuric acid and new ^{195}Pt NMR data about "putative" $[\text{Pt}(\text{H}_2\text{O})_6]^{4+}$ ion.^{36–38} Because of the impossibility to measure the degree of $[\text{Pt}(\text{H}_2\text{O})_6]^{4+}$ dissociation in the acidic solutions exactly, we use the designation "L" for both H_2O and OH ligands and no charge signs for complexes containing these ligands are used throughout the paper.

After dissolution of $\text{H}_2[\text{Pt}(\text{OH})_6]$ in acids, besides "main" signal of $[\text{Pt}(\text{L})_6]$, an additional weak signal at ~ 3590 ppm appears in the NMR spectra. A similar signal (3570 ppm) was observed in the solution of $\text{PtO}_2 \cdot 3\text{H}_2\text{O}$ in 1 M NaOH and in basic solutions of $\text{H}_2[\text{Pt}(\text{OH})_6]$.^{18,29} The authors have attributed this signal to OH-bridged complex of Pt(IV), probably $[(\text{OH})_4\text{Pt}(\mu\text{-OH})_2\text{Pt}(\text{OH})_4]^{2-}$. In our acidic solution, we assign the signal at 3590 ppm to corresponding neutral or positively charged $[(\text{L})_4\text{Pt}(\mu\text{-OH})_2\text{Pt}(\text{L})_4]$ molecules. Such species either contained in $\text{H}_2[\text{Pt}(\text{OH})_6]$ initially or formed during its dissolution in acids. Under acidic conditions the OH-bridged complex can undergo a breakdown through protonation of bridged OH-ligands to form a monomeric $[\text{Pt}(\text{L})_6]$ complex.

Complexes of Pt(IV) with Nitrate Ions. After dissolution of $\text{H}_2[\text{Pt}(\text{OH})_6]$ in nitric acid the NO_3^- anions can substitute L ligands in $[\text{Pt}(\text{L})_6]$. There are three signals in the ^{195}Pt NMR spectrum of freshly prepared $\text{H}_2[\text{Pt}(\text{OH})_6]$ solution in 15.8 M nitric acid corresponding to $[\text{Pt}(\text{L})_6]$, $[\text{Pt}_2(\mu\text{-OH})_2(\text{L})_8]$ and $[\text{Pt}(\text{L})_5(\text{NO}_3)]$ (3444 ppm) species. Signals of all 10 aqua-nitrate complexes (Scheme 1) arise within 1 h after preparation of the solution (297 K). They appear in weaker fields, relative to the initial $[\text{Pt}(\text{L})_6]$ complex at regular intervals (~ 100 ppm), according to the numbers of coordinated NO_3^- ions (if signals of geometric isomers are averaged). Typical spectrum is shown in Figure 2. In parallel with the substitution process, breakdown of the dimeric $[\text{Pt}_2(\mu\text{-OH})_2(\text{L})_8]$ complex occurs as a result of its protonation or (and) anation, and after an hour, its signal disappears completely.

Scheme 1. Reaction Scheme for the Stepwise Replacement of “L”-Ligands ($L = \text{H}_2\text{O}$ or OH^-) with Nitrate Ions in $[\text{PtL}_6]$ and the Designations of Species

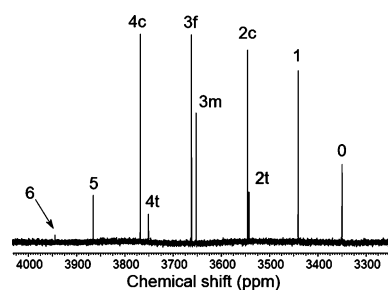
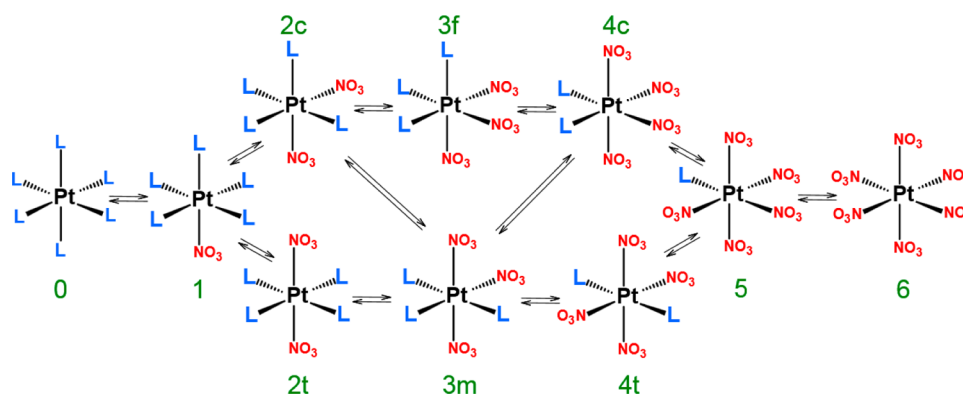


Figure 2. ^{195}Pt NMR spectrum of $\text{H}_2[\text{Pt}(\text{OH})_6]$ solution in 15.8 M HNO_3 , 60 min after preparation, $T = 297$ K. Numbers correspond to x values of $[\text{Pt}(\text{L})_{6-x}(\text{NO}_3)_x]$ species ($L = \text{H}_2\text{O}$ or OH^-). See Scheme 1 for the complex designations.

The substitution process has a surprisingly high rate for complexes of the d^6 $\text{Pt}(\text{IV})$ ion, which is known to be kinetically quite inert. At ambient temperature (297 K), equilibration of monomeric aqua-nitrato complexes was achieved ~ 6 h after preparation of the solution.

We assigned signals of expected geometric isomers pairs based on the fact that intensity ratios after equilibration are close to the statistically expected ratios for $\text{cis-}[\text{Pt}(\text{L})_4(\text{NO}_3)_2]$ to $\text{trans-}[\text{Pt}(\text{L})_4(\text{NO}_3)_2]$ (calc. 4:1, found 4.1:1), $\text{fac-}[\text{Pt}(\text{L})_3(\text{NO}_3)_3]$ to $\text{mer-}[\text{Pt}(\text{L})_3(\text{NO}_3)_3]$ (calc. 2:3, found 2:2.7), and $\text{trans-}[\text{Pt}(\text{L})_2(\text{NO}_3)_4]$ to $\text{cis-}[\text{Pt}(\text{L})_2(\text{NO}_3)_4]$ (calc. 1:4, found 1:3.4) (see Table 2).

Thus, in concentrated (15.8 M) nitric acid, substitution of the “L”-ligand by the NO_3^- ion at a position *trans* to another “L”-ligand causes a larger change in chemical shift ($\Delta\delta \approx 116$ ppm) than the substitution of “L”-ligand at a position *trans* to a NO_3^- ion ($\Delta\delta \approx 105$ ppm).

Observed spectral pattern can be expressed by pair additivity model of chemical shifts.^{39,40} $\delta(^{195}\text{Pt})$ $[\text{Pt}(\text{L})_6]$ complex was taken as the origin (0 ppm) and chemical shift of each $[\text{Pt}(\text{L})_{6-x}(\text{NO}_3)_x]$ complex was expressed in terms of ligands interaction increments:

$$\delta = \sum_{i,j} c_{ij} \eta_{ij} \quad (2)$$

where η_{ij} expresses the pair arrangement of ligands in a coordination sphere of $\text{Pt}(\text{IV})$: $(\text{L}-\text{L})_{\text{cis}}$, $(\text{L}-\text{NO}_3)_{\text{cis}}$, $(\text{NO}_3-\text{NO}_3)_{\text{cis}}$, $(\text{L}-\text{L})_{\text{trans}}$, $(\text{L}-\text{NO}_3)_{\text{trans}}$, $(\text{NO}_3-\text{NO}_3)_{\text{trans}}$, and c_{ij} are numbers of such interactions ij in each particular complex. For example, for $\text{mer-}[\text{Pt}(\text{L})_3(\text{NO}_3)_3]$, the following expression can be concluded:

$$\delta = (\text{L}-\text{L})_{\text{trans}} + (\text{NO}_3-\text{NO}_3)_{\text{trans}} + (\text{L}-\text{NO}_3)_{\text{trans}} + 2(\text{L}-\text{L})_{\text{cis}} + 2(\text{NO}_3-\text{NO}_3)_{\text{cis}} + 8(\text{L}-\text{NO}_3)_{\text{cis}}$$

where the coefficients 1, 1, 1, 2, 2, and 8 are c_{ij} . Both $(\text{L}-\text{L})_{\text{cis}}$ and $(\text{L}-\text{L})_{\text{trans}}$ increments are equal to zero, because, for $[\text{Pt}(\text{L})_6]$, $\delta(^{195}\text{Pt}) = 0$.

Minimization of differences between 12 experimental and 12 calculated chemical shift values by least-squares treatment was used to find optimum values of η_{ij} . Calculation results and assignment of signals in the ^{195}Pt NMR spectrum are represented in Table 2.

Within the pair additivity model, the difference between chemical shifts of geometric isomers is a constant and can be expressed as

$$\Delta\delta = (\text{NO}_3-\text{NO}_3)_{\text{cis}} + 2(\text{L}-\text{NO}_3)_{\text{trans}} - 2(\text{L}-\text{NO}_3)_{\text{cis}} - (\text{NO}_3-\text{NO}_3)_{\text{trans}} \quad (3)$$

Table 2. ^{195}Pt Chemical Shift Assignments of All $[\text{Pt}(\text{L})_{6-x}(\text{NO}_3)_x]$ ($L = \text{H}_2\text{O}$ or OH^- ; $x = 0-6$) Complexes in 15.8 M Nitric Acid Solution ($C_{\text{Pt}} = 0.5$ M): Experimental and Calculated from Pair Additivity Model Values

complex	Chemical Shift (ppm)		complex	Chemical Shift (ppm)	
	experimental	calculated ^a		experimental	calculated ^a
$[\text{Pt}(\text{L})_6]$	3352	3352	$\text{fac-}[\text{Pt}(\text{L})_3(\text{NO}_3)_3]$	3670	3675
$[\text{Pt}(\text{L})_5(\text{NO}_3)]$	3444	3458	$\text{trans-}[\text{Pt}(\text{L})_2(\text{NO}_3)_4]$	3760	3756
$\text{trans-}[\text{Pt}(\text{L})_4(\text{NO}_3)_2]$	3547	3552	$\text{cis-}[\text{Pt}(\text{L})_2(\text{NO}_3)_4]$	3780	3770
$\text{cis-}[\text{Pt}(\text{L})_4(\text{NO}_3)_2]$	3549	3566	$[\text{Pt}(\text{L})(\text{NO}_3)_5]$	3882	3867
$\text{mer-}[\text{Pt}(\text{L})_3(\text{NO}_3)_3]$	3659	3660	$[\text{Pt}(\text{NO}_3)_6]^{2-}$	3940	3964

^a $(\text{L}-\text{NO}_3)_{\text{cis}} = 24.6$, $(\text{NO}_3-\text{NO}_3)_{\text{cis}} = 50.3$, $(\text{L}-\text{NO}_3)_{\text{trans}} = 8.2$, $(\text{NO}_3-\text{NO}_3)_{\text{trans}} = 3.0$ ppm.

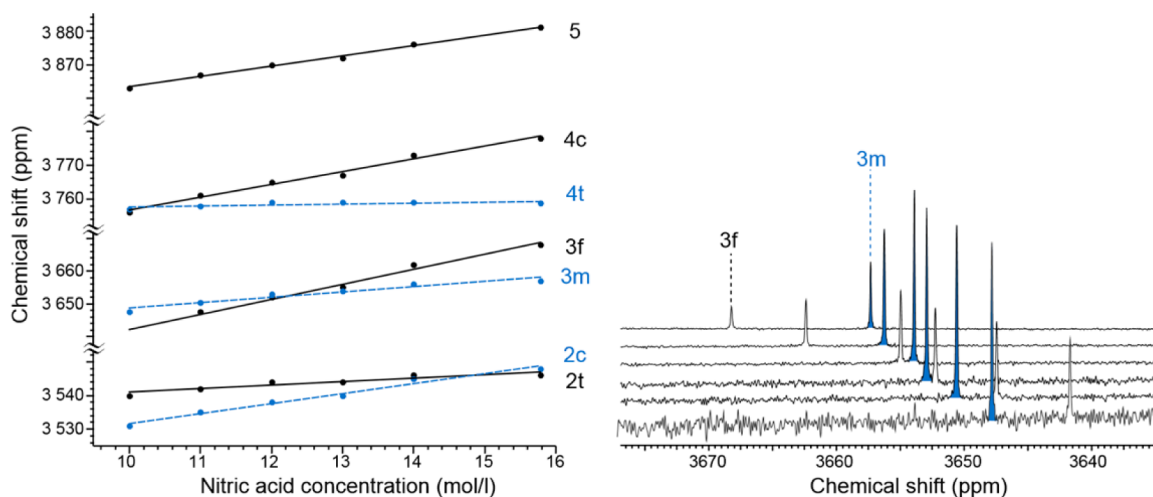


Figure 3. (a) Dependence of $[\text{Pt}(\text{L})_{6-x}(\text{NO}_3)_x]$ ($\text{L} = \text{H}_2\text{O}$ or OH^-) complexes ^{195}Pt NMR chemical shifts on nitric acid concentration. (b) Representation of the same dependence for *fac*- $[\text{Pt}(\text{L})_3(\text{NO}_3)_3]$ and *mer*- $[\text{Pt}(\text{L})_3(\text{NO}_3)_3]$ complexes as a stack of ^{195}Pt NMR spectra. See Scheme 1 for designations.

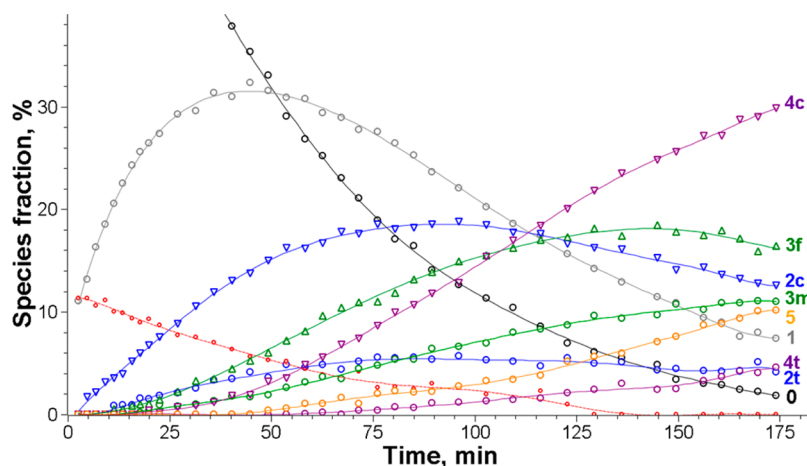


Figure 4. Dynamic of monomeric $[\text{Pt}(\text{L})_{6-x}(\text{NO}_3)_x]$ ($\text{L} = \text{H}_2\text{O}$ or OH^-) species distribution in the solution of $\text{H}_2[\text{Pt}(\text{OH})_6]$ in 15.8 M HNO_3 during 3 h from preparation, $T = 278$ K. See Scheme 1 for designations; red line corresponds to data for the dimeric complex $[\text{Pt}_2(\mu\text{-OH})_2(\text{L})_8]$.

Deviations of the experimental $\Delta\delta$ values from the calculated ones can be attributed to nonequivalence of “L”-ligands in different complexes. Substitution of the “L”-ligand by the NO_3^- ion decreases the total charge and acidity of the coordinated water molecule. In other words, the degree of protonation of “L” is altered through the substitution process and with increasing x in $[\text{Pt}(\text{L})_{6-x}(\text{NO}_3)_x]$, “L”-ligands in the platinum inner sphere become closer to H_2O than to OH^- .

It correlates well with experimental facts that the signals of Pt(IV) species shift differently when the HNO_3 content in the solutions is varied. Increasing the HNO_3 concentration from 6 M to 15.8 M results in an exchange of relative positions of geometric isomers signals (Figure 3). These results suggest that the degree of protonation of “L” is altered with variation of the HNO_3 concentration, and, in concentrated nitric acid (15.8 M), “L”-ligands in the complexes become closer to H_2O than to OH^- . A similar exchange of signals positions was noticed by Goodfellow and co-workers for $[\text{PtCl}_{6-n}(\text{OH})_n]^{2-}$ and $[\text{PtCl}_n(\text{H}_2\text{O})_{6-n}]^{4-n}$ as the solution acidity decreased from pH 10–12 to pH 1–3.⁴¹

Because of the high rate of the substitution reactions, it was difficult to study their dynamics by ^{195}Pt NMR spectroscopy.

Therefore, we have monitored these processes at lower temperature (278 K). The overall transformation pattern (Figure 4) represents rapid consumption of the $[\text{Pt}(\text{L})_6]$ species and, after 60 min, $[\text{Pt}(\text{L})_5\text{NO}_3]$ becomes dominant. Further substitution process results in a prevalence of tetra(nitrato) and tri(nitrato) complexes in the solution after 3 h. Raman spectra of the solutions during this time (3 h) show peaks at 770 and 560 cm^{-1} , corresponding to coordinated NO_3^- and H_2O and a strong peak at 340 cm^{-1} referred to the $\{\text{PtO}_6\}$ octahedron stretching vibrations (see Figure 5).

Platinum(IV) speciation in the equilibrated solutions exhibits a clear dependence on the nitric acid concentration (see Figure 6). The increase in concentration of HNO_3 results in shift of Pt(IV) speciation to the penta(nitrato) and hexa(nitrato) complexes, but even in 15.8 M HNO_3 , the fraction of $[\text{Pt}(\text{NO}_3)_6]^{2-}$ is only 10%.

Crystallization of $(\text{PyH})_2[\text{Pt}(\text{NO}_3)_6]$. The addition of pyridine to concentrated nitric acid causes further increases in the NO_3^- concentration, because of the equilibrium shift and pyridinium-ion formation. As the concentration of the ionic nitrate increases, the shares of hexa(nitrato) and penta(nitrato) complexes grow, whereas the shares of others complexes fall.

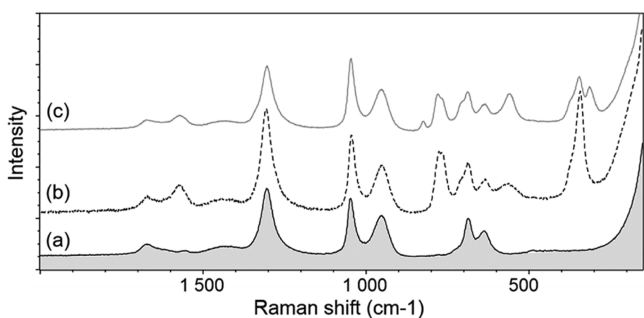


Figure 5. Raman spectra of (a) concentrated nitric acid 15.8 M, (b) a freshly prepared solution of $\text{H}_2[\text{Pt}(\text{OH})_6]$ in 15.8 M HNO_3 , $C_{\text{Pt}} = 0.5$ M, and (c) the same solution after 24 h.

Slow evaporation of $\text{H}_2[\text{Pt}(\text{OH})_6]$ solution in such HNO_3 – H_2O – Py mixture yields pale yellow crystals of $(\text{PyH})_2[\text{Pt}(\text{NO}_3)_6]$ in a good yield. This compound quickly hydrolyzes in water but can be dissolved without decomposition in concentrated nitric acid or acetone.

In the structure of $(\text{PyH})_2[\text{Pt}(\text{NO}_3)_6]$, the platinum center has the coordination environment formed by six O atoms of monodentately coordinated nitrate ions (Figure 7). The resulting $\{\text{PtO}_6\}$ polyhedron is a trigonal antiprism (D_{3d}) and the Pt center is located on an inversion point of the unit cell. The geometric characteristics of the $[\text{Pt}(\text{NO}_3)_6]^{2-}$ anions (Table 3) are almost identical to those previously observed in $(\text{NO})_2[\text{Pt}(\text{NO}_3)_6]$ salt.¹⁶

Oligomerization of the Nitrate Complexes. After 6–7 h at ambient temperature, another process begins to be detectable in the spectra (15.8 M HNO_3 , $C_{\text{Pt}} = 0.5$ M). New groups of signals appear and begin to grow in a downfield range of 4000–4500 ppm. This process, being quite slow, was monitored with 85% ^{195}Pt enriched samples over a period of 24 h. No noticeable change in the spectra was observed after approximately two weeks (see Figure 8).

There are two types of new signals: pairs of multiline sets of signals with the same structure and equal intensity, and singlet signals. Observed splitting constant for the multiline sets of signals is ~ 600 – 700 Hz. The nuclei of nitrogen and hydrogen must be directly connected with platinum(IV) to provide such a splitting value, but the formation of appropriate species (NO_2^- , NH_3 , H^-) seems to be unlikely in our case. The natural

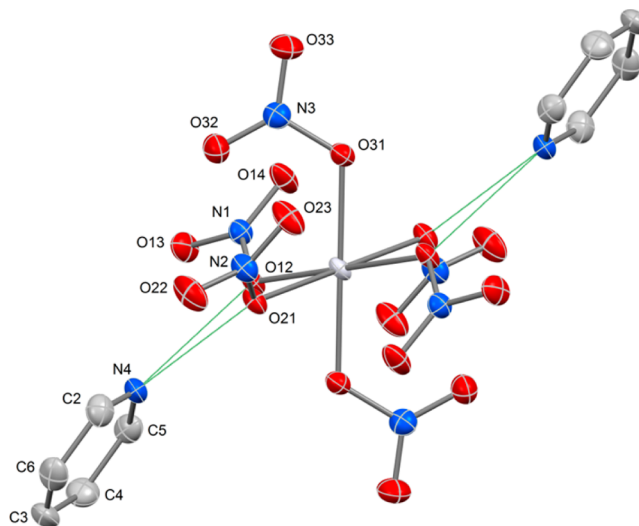


Figure 7. Molecular structure of $(\text{PyH})_2[\text{Pt}(\text{NO}_3)_6]$ (ORTEP presentation at 30% probability of the depicted atoms and atom numbering scheme). H atoms are omitted for the sake of clarity. Hydrogen bonds are shown with green lines.

Table 3. Selected Geometric Parameters for the $[\text{Pt}(\text{NO}_3)_6]^{2-}$ Anion in the Structure of $(\text{PyH})_2[\text{Pt}(\text{NO}_3)_6]$

Bond Distances (Å)		Bond Angles (deg)	
Pt(1)–O(11)	2.0076(14)	N(3)–O(31)–Pt(1)	121.53(11)
Pt(1)–O(21)	2.0107(15)	O(13)–N(1)–O(14)	126.76(18)
Pt(1)–O(31)	2.0123(14)	O(13)–N(1)–O(11)	113.65(16)
N(1)–O(11)	1.346(2)	O(14)–N(1)–O(11)	119.58(16)
N(1)–O(14)	1.217(2)	N(2)–O(21)–Pt(1)	120.50(12)
N(1)–O(13)	1.213(2)	O(23)–N(2)–O(22)	126.3(2)
N(2)–O(21)	1.335(2)	O(23)–N(2)–O(21)	119.85(18)
N(2)–O(22)	1.221(2)	O(22)–N(2)–O(21)	113.87(18)
N(2)–O(23)	1.209(2)	O(32)–N(3)–O(33)	126.87(19)
N(3)–O(31)	1.351(2)	O(32)–N(3)–O(31)	119.37(17)
N(3)–O(32)	1.209(2)	O(33)–N(3)–O(31)	113.76(17)
N(3)–O(33)	1.216(2)	N(1)–O(11)–Pt(1)	121.94(11)

abundance of magnetically active isotopes of ^{17}O is too low (0.038%). The only appropriate nucleus being ^{195}Pt , we have assigned these new signals to oligonuclear aqua-nitrato complexes of Pt(IV). It should be noted that platinum has

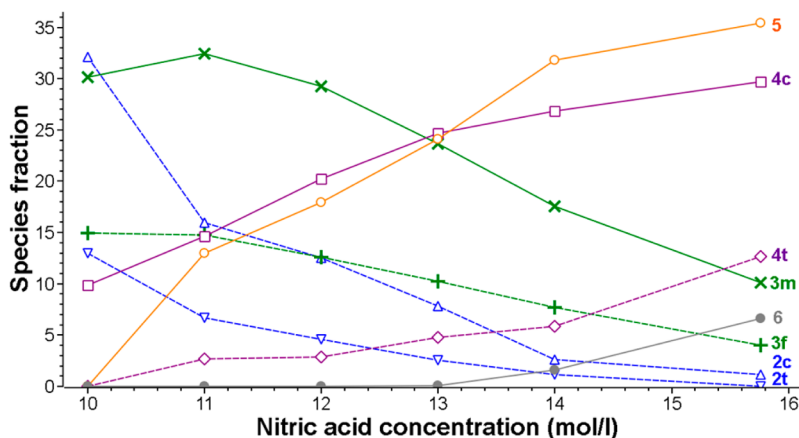


Figure 6. Dependence of monomeric $[\text{Pt}(\text{L})_{6-x}(\text{NO}_3)_x]$ ($\text{L} = \text{H}_2\text{O}$ or OH^-) species distribution on concentration of HNO_3 in the solution (based on ^{195}Pt NMR data). See Scheme 1 for designations.

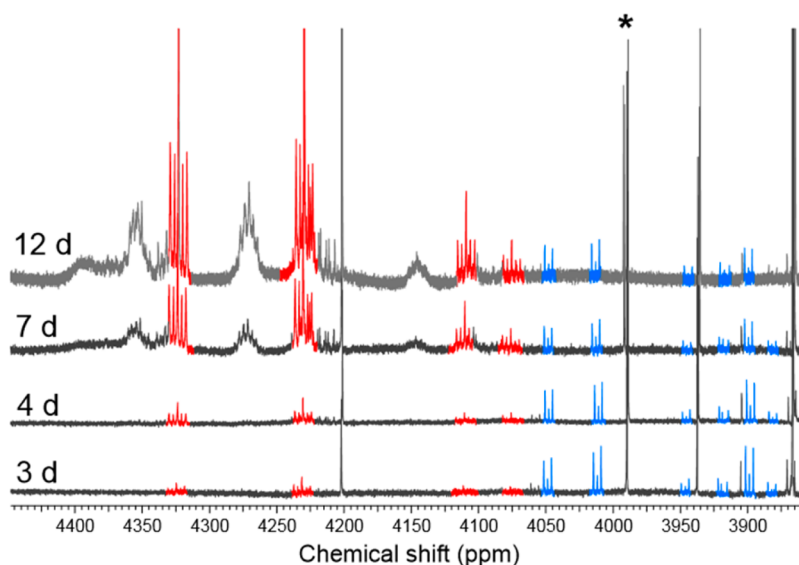


Figure 8. Changes in ^{195}Pt NMR spectrum of $\text{H}_2[\text{Pt}(\text{OH})_6]$ nitric acid solution over time (85% ^{195}Pt enriched sample, 15.8 M HNO_3). Color labels mark multiplet signals of AX (blue) and A_2X_2 (red) systems. The signal of $[\text{Pt}_2(\mu\text{-OH})_2(\text{NO}_3)_8]^{2-}$ is marked with an asterisk (*).

only one NMR active isotope (^{195}Pt , $I = 1/2$) with natural abundance of 33.8%, and to study the polynuclear species, we also used an isotopically enriched sample of $\text{H}_2[\text{Pt}(\text{OH})_6]$ (85% ^{195}Pt).

Two forms of multiline sets of signals are clearly observed in the spectra (3800–4400 ppm region): three-line and five-line sets. Intensities of the lines in the sets relate approximately as 1:4:1 and 1:8:18:8:1 in the spectra with natural abundance, and 3:1:3 and 1:1:3:1:1 in the spectra of isotopically enriched sample (see Figure 9). Analysis of these sets with gNMR software⁴² revealed that the signals were fitted well as spectra of AX and A_2X_2 systems correspondingly for the three-line and five-line sets (where A and X are magnetically nonequivalent Pt nuclei). Spectrum of A (or X) in the AX system is the sum of

two subspectra derived from species AX (doublet) and AX^* (singlet), where X^* is a magnetically inactive Pt isotope. Analogously, for the A_2X_2 system, where each A connected with two X and vice versa, the spectrum of A is the sum of three subspectra from species AX_2 (triplet), AX^*X (doublet), and AX_2^* (singlet).

From the chemical point of view, the AX and A_2X_2 systems correspond to binuclear and tetranuclear aqua-nitrato complexes of Pt(IV) with two types of coordination environment of platinum atoms connected by NO_3^- or OH-bridged groups. If all Pt nuclei in polynuclear species have identical environments ($\text{A} \equiv \text{X}$), then their NMR signal is a singlet. We observed similar strong singlets at 3990 and 4200 ppm, for example. In addition, poorly resolved sets of signals (4130, 4270, 4350, 4380 ppm) were observed, which can be derived from more-complicated oligomeric aqua-nitrato complexes with the number of nuclei being >4.

Similar ^{195}Pt NMR spectra with multiline sets of signals were observed for polynuclear Pt(II,IV) oxo-nitro complexes,⁴³ and for platinum cluster complexes with CO and phosphines.^{44,45} Moreover, the Pt–O–Pt splitting constants found for Pt(II,IV) oxo-nitro complexes with oxo- and hydroxo-bridged platinum ions are very close (630–780 Hz) to be observed in our spectra.

New peaks arise in Raman spectra of the solutions after aging (24 h), as compared with fresh prepared solutions (Figure 4). These new peaks can be attributed to vibrations of bridged NO_3^- ligands (824 cm^{-1}) and stretching vibrations of Pt–O–Pt bridges in oligonuclear species (315 cm^{-1}).

Crystallization of $(\text{Me}_4\text{N})_2[\text{Pt}_2(\mu\text{-OH})_2(\text{NO}_3)_8]$. Evaporation of the “platinum nitrate” solution with the addition of tetramethylammonium nitrate yields crystals of the dimeric complex $(\text{Me}_4\text{N})_2[\text{Pt}_2(\mu\text{-OH})_2(\text{NO}_3)_8]$. To the best of our knowledge, this is the first example of a bis(μ -hydroxo) complex of platinum(IV) in a purely oxygen environment (see Figure 10).

X-ray analysis reveals that the dimeric complex has a centrosymmetric structure with two distorted PtO_6 edge-sharing octahedra. The environment of the Pt atoms is a trigonal antiprism distorted due to the nonequivalence of Pt–O

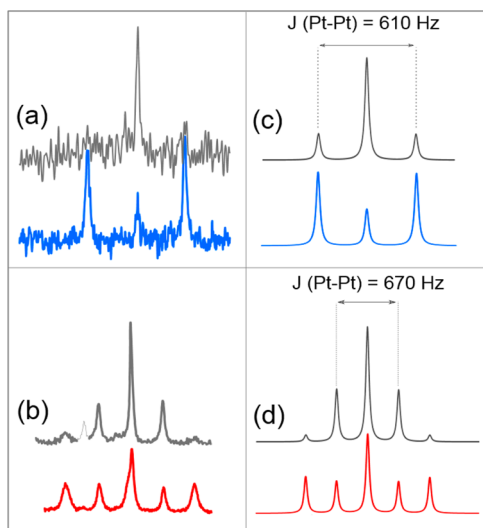


Figure 9. Experimental (left) and calculated (right) ^{195}Pt NMR three-line and five-line sets of signals referred to (a, c) the AX system and (b, d) the A_2X_2 system. Experimental data correspond to the sets of signals centered at (a) 4010 ppm and (b) 4325 ppm. Gray lines represent natural abundance spectra; colored lines represent the spectra of isotopically enriched samples.

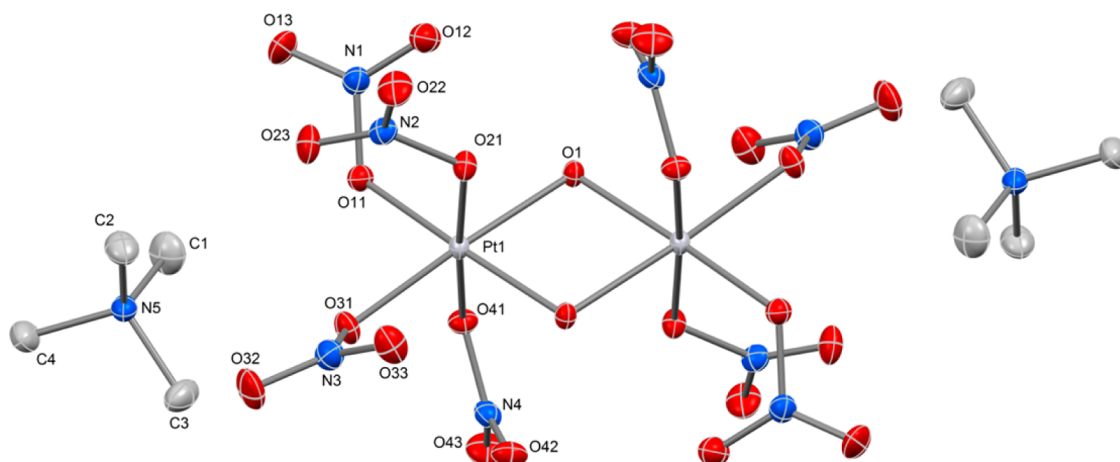


Figure 10. Molecular structure of $(\text{Me}_4\text{N})_2[\text{Pt}_2(\mu\text{-OH})_2(\text{NO}_3)_8]$ (ORTEP presentation at 30% probability of the depicted atoms and atom numbering scheme). H atoms omitted for the sake of clarity.

bonds (see Table 4). The geometric parameters of the Pt_2O_2 ring [Pt—O, 2.03 Å; Pt···Pt, 3.12 Å; O—Pt—O, 79.53°; and Pt—O—Pt, 100.47°] are not significantly different from the values found in bis(μ -hydroxo) dimers of Pt(II) and Pt(IV).^{46–48} Complex anions $[\text{Pt}_2(\mu\text{-OH})_2(\text{NO}_3)_8]^{2-}$ are connected together by a system of hydrogen bonds with O···O distances falling in the narrow range of 2.979–3.025 Å.

Table 4. Selected Geometric Parameters for $[\text{Pt}_2(\mu\text{-OH})_2(\text{NO}_3)_8]^{2-}$ Anion^a

Bond Distances (Å)			
Pt1—O31	1.9892(18)	O41—N4	1.349(2)
Pt1—O21	2.0001(17)	O21—N2	1.361(2)
Pt1—O11	2.0014(16)	O11—N1	1.370(3)
Pt1—O41	2.0037(17)	O23—N2	1.217(3)
Pt1—O1	2.0280(16)	O33—N3	1.204(3)
Pt1—O1 ⁱ	2.0312(17)	O32—N3	1.215(3)
Pt1—Pt1 ⁱ	3.1206(2)	O42—N4	1.221(3)
O1—Pt1 ⁱ	2.0312(17)	O43—N4	1.216(3)
O31—N3	1.364(3)	O22—N2	1.213(3)
O12—N1	1.228(3)	N1—O13	1.204(3)
Bond Angles (deg)			
O41—Pt1—O1 ⁱ	87.44(7)	O22—N2—O23	126.9(2)
O1—Pt1—O1 ⁱ	79.52(7)	O22—N2—O21	113.9(2)
O31—Pt1—Pt1 ⁱ	141.27(5)	O23—N2—O21	119.2(2)
O21—Pt1—Pt1 ⁱ	82.78(5)	O43—N4—O42	126.0(2)
O11—Pt1—Pt1 ⁱ	136.73(5)	O43—N4—O41	113.92(19)
O41—Pt1—Pt1 ⁱ	93.42(5)	O42—N4—O41	120.1(2)
O1—Pt1—Pt1 ⁱ	39.79(5)	O31—Pt1—O21	100.19(7)
O1 ⁱ —Pt1—Pt1 ⁱ	39.72(5)	O31—Pt1—O11	81.11(7)
Pt1—O1—Pt1 ⁱ	100.49(7)	O21—Pt1—O11	100.77(7)
N3—O31—Pt1	120.80(15)	O31—Pt1—O41	84.95(7)
N4—O41—Pt1	121.68(14)	O21—Pt1—O41	174.85(7)
N2—O21—Pt1	119.96(14)	O11—Pt1—O41	79.60(7)
N1—O11—Pt1	118.73(14)	O31—Pt1—O1	101.98(7)
O13—N1—O12	127.6(2)	O21—Pt1—O1	81.48(7)
O13—N1—O11	113.7(2)	O11—Pt1—O1	175.86(7)
O12—N1—O11	118.6(2)	O41—Pt1—O1	97.84(7)
O33—N3—O32	128.1(2)	O31—Pt1—O1 ⁱ	172.38(7)
O33—N3—O31	118.9(2)	O21—Pt1—O1 ⁱ	87.41(7)
O32—N3—O31	112.9(2)	O11—Pt1—O1 ⁱ	97.06(7)

^aSymmetry code: (i) $-x + 1, -y, -z + 2$.

The ^{195}Pt NMR spectrum of $(\text{Me}_4\text{N})_2[\text{Pt}_2(\mu\text{-OH})_2(\text{NO}_3)_8]$ in acetone shows the single resonance at ~ 4000 ppm that agrees well with the location of the singlet signal in the spectrum of the “platinum nitrate” solution (3990 ppm). Dissolution of the compound in nitric acid results in nitrate ligands substitution (presumably by water) and signals of unsymmetrical dimers (triplets) appear in the NMR spectrum (see Figure S1 in the Supporting Information).

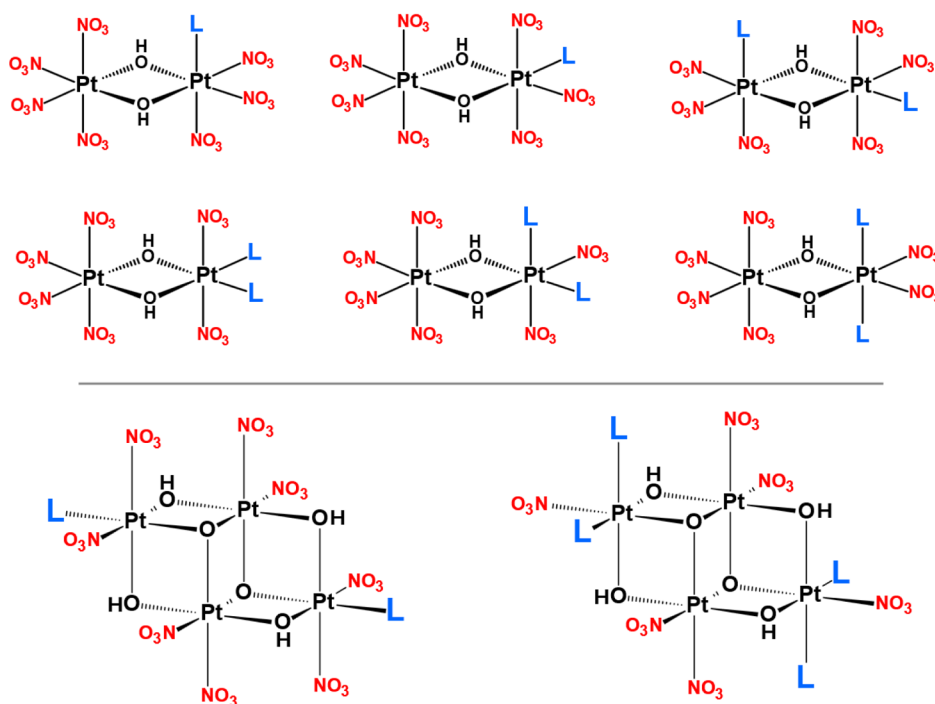
Possible structures of unsymmetrical dimeric complexes (AX) corresponding to the three-line sets of signals in the ^{195}Pt NMR spectra can be suggested as products of NO_3^- ions substitution by L in symmetrical $[\text{Pt}_2(\mu\text{-OH})_2(\text{NO}_3)_8]^{2-}$ anions. Analogously, models of tetrameric (A_2X_2) complexes can be hypothesized (see Scheme 2). Mentioned models, of course, do not cover all diversity of platinum oligonuclear species in the “platinum nitrate” solutions (complexes with bridging NO_3^- groups are possible, for example) but serve as a reference for further, more-detailed explorations.

CONCLUSION

In the present work, complexation of Pt(IV) with NO_3^- anions in a nitric acid medium has been studied by NMR and Raman spectroscopy. We found that two sets of platinum(IV) complexes form in such solutions: monomeric aqua-hydroxo-nitrato complexes $[\text{Pt}(\text{L})_{6-x}(\text{NO}_3)_x]$ ($\text{L} = \text{H}_2\text{O}$ or OH^-) and oligomeric complexes with the same ligands. The first set of complexes prevails in the solution during first 6–7 h from the preparation moment. After this period, condensation of monomeric species to oligomeric ones begins to be detectable and this second set of complexes slowly (several days) becomes dominant.

The addition of organic cations (PyH^+ , Me_4N^+), followed by evaporation of the solutions, cause selective crystallization of salts containing the hexa(nitrato)platinum anion or the dimeric anion $[\text{Pt}_2(\mu\text{-OH})_2(\text{NO}_3)_8]^{2-}$. It should be noted that these complexes are not dominant species in the nitric acid solutions, and the good yield of the crystallization is a consequence of the stability of corresponding solid phases. Therefore, other mononuclear and polynuclear aqua-hydroxo-nitrato complexes of platinum(IV) can be isolated with various cations from nitric acid solutions, and such work is underway in our laboratory.

Scheme 2. Some Possible Structures of Unsymmetrical Dimeric and Tetrameric Complexes Corresponding to AX and A_2X_2 Systems in the ^{195}Pt NMR Spectra ($L = \text{H}_2\text{O}$ or OH^-)



■ ASSOCIATED CONTENT

■ Supporting Information

X-ray crystallographic data for $(\text{PyH})_2[\text{Pt}(\text{NO}_3)_6]$ and $(\text{Me}_4\text{N})_2[\text{Pt}_2(\mu\text{-OH})_2(\text{NO}_3)_8]$ in CIF format. Further details may be obtained from the Cambridge Crystallographic Data Center upon quoting depository numbers CCDC 926762 and 929104. Copies of this information may be obtained free of charge from <http://www.ccdc.cam.ac.uk>. ^{195}Pt NMR spectra of $(\text{Me}_4\text{N})_2[\text{Pt}_2(\mu\text{-OH})_2(\text{NO}_3)_8]$ in (a) nitric acid and (b) acetone solutions are represented in Figure S1. This material is available free of charge via the Internet at <http://pubs.acs.org>.

■ AUTHOR INFORMATION

Corresponding Author

*E-mail: vasilchenko@niic.nsc.ru.

Notes

The authors declare no competing financial interest.

■ ACKNOWLEDGMENTS

We thank Drs. A. V. Belyaev and A. B. Venediktov for helpful discussion. This work was supported by "The Gulidov Krasnoyarsk Non-Ferrous Metals Plant" Open Joint Stock Company.

■ REFERENCES

- (1) Gillard, R. D.; Hanton, L. R.; Mitchell, S. H. *Polyhedron* **1990**, *9*, 2127–2133.
- (2) Gaunt, A. J.; May, I.; Neu, M. P.; Reilly, S. D.; Scott, B. L. *Inorg. Chem.* **2011**, *50*, 4244–4246.
- (3) Bradley, A. E.; Hatter, J. E.; Nieuwenhuyzen, M.; Pitner, W. R.; Seddon, K. R.; Thied, R. C. *Inorg. Chem.* **2002**, *41*, 1692–1694.
- (4) Khalil, M. I.; Logan, N.; Harris, A. D. *J. Chem. Soc., Dalton Trans.* **1980**, 314–316.
- (5) Caminiti, R.; Atzei, D.; Cucca, P.; Anedda, A.; Bongiovanni, G. *J. Phys. Chem.* **1986**, *90*, 238–243.

- (6) Canagaratna, M.; Phillips, J. A.; Ott, M. E.; Leopold, K. R. *J. Phys. Chem. A* **1998**, *102*, 1489–1497.
- (7) Gasser, G.; Belousoff, M. J.; Bond, A. M.; Spiccia, L. *Inorg. Chem.* **2007**, *46*, 3876–88.
- (8) Gradeff, P. S.; Yunlu, K.; Deming, T. J.; Olofson, J. M.; Ziller, J. W.; Evans, W. J. *Inorg. Chem.* **1989**, *28*, 2600–2604.
- (9) Fanning, J. C.; Resce, J. L.; Lickfield, G. C.; Kotun, M. E. *Inorg. Chem.* **1985**, *24*, 2884–2889.
- (10) Critchlow, P. B.; Robinson, S. D. *Inorg. Chem.* **1978**, *17*, 1896–1901.
- (11) Wickleder, M. S.; Büchner, O.; Gerlach, F.; Necke, M.; Al-Shamery, K.; Wich, T.; Luttermann, T. *Chem. Mater.* **2008**, *20*, 5181–5185.
- (12) Kolarik, Z.; Renard, E. V. *Platinum Met. Rev.* **2003**, *47*, 74–87.
- (13) Kolarik, Z.; Renard, E. V. *Platinum Met. Rev.* **2003**, *47*, 123–131.
- (14) Addison, C. C. *Chem. Rev.* **1980**, *80*, 21–39.
- (15) Harrison, B.; Logan, N. J. *Chem. Soc., Dalton Trans.* **1972**, 1587–1589.
- (16) Harrison, B.; Logan, N.; Raynor, J. B. *J. Chem. Soc., Chem. Commun.* **1974**, 202–203.
- (17) Wickleder, M. S.; Gerlach, F.; Gagelmann, S.; Bruns, J.; Fenske, M.; Al-Shamery, K. *Angew. Chem., Int. Ed.* **2012**, *51*, 2199–2203.
- (18) Appleton, T. G.; Hall, J. R.; Ralph, S. F.; Thompson, C. S. M. *Inorg. Chem.* **1984**, *23*, 3521–3525.
- (19) Elding, L. I.; Oskarsson, Å. *Inorg. Chim. Acta* **1985**, *103*, 127–131.
- (20) Scott, H. G. *Acta Crystallogr., Sect. B: Struct. Crystallogr. Cryst. Chem.* **1979**, *B35*, 3014–3015.
- (21) Foster, A. J.; Do, P. T. M.; Lobo, R. F. *Top. Catal.* **2012**, *55*, 118–128.
- (22) Ohtsuka, H. *Catal. Lett.* **2011**, *141*, 413–419.
- (23) Reddy, B. M.; Rao, K. N.; Reddy, G. K. *Catal. Lett.* **2009**, *131*, 328–336.
- (24) Dawody, J.; Tönnies, I.; Fridell, E.; Skoglundh, M. *Top. Catal.* **2007**, *42–43*, 183–187.
- (25) Kim, D.; Kung, M.; Kozlova, A.; Yuan, S.; Kung, H. *Catal. Lett.* **2004**, *98*, 11–15.
- (26) Ravenelle, R. M.; Copeland, J. R.; Pelt, A. H.; Crittenden, J. C.; Sievers, C. *Top. Catal.* **2012**, *55*, 162–174.

- (27) Piermartini, P.; Schuhmann, T.; Pfeifer, P.; Schaub, G. *Top. Catal.* **2011**, *54*, 967–976.
- (28) Dou, D.; Liu, D.-J.; Williamson, W. B.; Kharas, K. C.; Robota, H. *J. Appl. Catal., B* **2001**, *30*, 11–24.
- (29) Beck, I. E.; Kriventsov, V. V.; Fedotov, M. A.; Bukhtiyarov, V. I. *Nucl. Instrum. Methods A* **2009**, *603*, 182–184.
- (30) Beck, I. E.; Kriventsov, V. V.; Ivanov, D. P.; Zaikovskiy, V. I.; Bukhtiyarov, V. I. *Nucl. Instrum. Methods A* **2009**, *603*, 108–110.
- (31) Belyaev, A. V.; Fedotov, M. A.; Vorobieva, S. N. *Russ. J. Coord. Chem.* **2011**, *37*, 281–287.
- (32) Venediktov, A. B.; Korenev, S. V.; Vasil'chenko, D. B.; Zadesenets, A. V.; Filatov, E. Y.; Mamonov, S. N.; Ivanova, L. V.; Prudnikova, N. G.; Semitut, E. Y. *Russ. J. Appl. Chem.* **2012**, *85*, 995–1002.
- (33) JCPDS Powder Diffraction File, Alphabetical Index, Inorganic Phases; International Centre for Diffraction Data (ICDD): Newtowne Square, PA, 1983.
- (34) Sheldrick, G. M. *Acta Crystallogr., Sect. A: Found. Crystallogr.* **2008**, *A64*, 112–122.
- (35) SADABS; Bruker AXS, Inc., Madison, WI, USA, 2001.
- (36) Simanova, S. A.; Nabivanets, B. I.; Kutsyi, V. G.; Kalabina, L. V.; Bashmakov, V. I. *Appl. Chem. USSR* **1990**, *63*, 419–422.
- (37) Richens, D. T. *The Chemistry of Aqua Ions*; John Wiley and Sons: New York, 1997.
- (38) Murray, P. A. *speciation study of various Pt(II) and Pt(IV) complexes including hexaaquaplatinum(IV) by means of ¹⁹⁵Pt NMR spectroscopy, in support of a preliminary study of the oxidation mechanism of various Pt(II) complexes*; Ph.D. Thesis, Stellenbosch University, Stellenbosch, South Africa, 2012.
- (39) Malinowski, E. R. *J. Am. Chem. Soc.* **1969**, *91*, 4701–4701.
- (40) Tarasov, V. P.; Privalov, V. I.; Buslaev, Y. A. *Mol. Phys.* **1978**, *35*, 1047–1055.
- (41) Carr, C.; Goggin, P. L.; Goodfellow, R. J. *Inorg. Chim. Acta* **1984**, *81*, L25–L26.
- (42) Budzelaar, P. H. M. *gNMR for Windows (5.0.6.0). NMR Simulation Program*, IvorySoft, Centennial, CO, USA, 2006.
- (43) Privalov, V. I.; Lapkin, V. V.; Tarasov, V. P.; Buslaev, Y. A. *Mendeleev Commun.* **1991**, *1*, 59–61.
- (44) Yudanov, V. F.; Eremenko, N. K.; Mednikov, E. G.; Gubin, S. P. *Z. Strukt. Khim.* **1984**, *25*, 49–52.
- (45) Moor, A.; Pregosin, P. S.; Venanzi, L. M.; Welch, A. J. *Inorg. Chim. Acta* **1984**, *85*, 103–110.
- (46) Al-Baker, S.; Vollano, J. F.; Dabrowiak, J. C. *J. Am. Chem. Soc.* **1986**, *108*, 5643–5644.
- (47) Rochon, F. D.; Guay, F. *Acta Crystallogr., Sect. C: Cryst. Struct. Commun.* **1987**, *C43*, 43–46.
- (48) Lopez, G.; Ruiz, J.; Garcia, G.; Vicente, C.; Marti, J. M.; Hermoso, J. A.; Vegas, A.; Martinez-Ripoll, M. *J. Chem. Soc., Dalton Trans.* **1992**, 53–58.